How much enhanced weathering carbon removal can croplands sustain?

Tyler Kukla[1,*], Zach Perzan[1,2], Connor Mack[3], Kate Maher[4], and Freya Chay[1]

[1]CarbonPlan, San Francisco, CA, USA
[2]Department of Geoscience, University of Nevada, Las Vegas, USA
[3]Scripps Institution of Oceanography, University of California San Diego, USA
[4]Department of Earth System Science, Stanford Doerr School of Sustainability, Stanford, California, USA
[*]Corresponding author: tyler@carbonplan.org

Abstract

Regional and global scoping models are the main quantitative basis for projections of gigaton-scale carbon dioxide removal (CDR) from enhanced weathering on croplands (EW). Their CDR fluxes often reach about 4–12 t ha^{-1} yr^{-1}, several times higher than long-term liming studies suggest croplands can sustain at near-neutral pH. Because CDR from EW generally rises with pH, and pushing pH too high can cause adverse agronomic effects, these fluxes raise the question of whether croplands can sustain them without alkalizing. Scoping models simplify EW's geochemistry to estimate CDR at large scales, and most do not track pH, leaving this question open. As a case study, we analyze the only scoping model we are aware of that reports the quantities needed to probe the carbonate chemistry linking CDR and pH. Closing the carbonate system reveals a trade-off: sustaining the model's CDR fluxes on U.S. croplands would push pH above 8 nearly everywhere, whereas holding pH near neutral reduces CDR by more than 80 percent. Because this trade-off is governed by carbonate chemistry, it broadly applies to scoping models that project high CDR fluxes. In soils, buffering by reserve acidity can obscure this trade-off, dampening the pH response to weathering by neutralizing alkalinity that could otherwise become CDR. Models that omit this alkalinity loss, or do not simulate the pH response to EW, risk overestimating the CDR that croplands can sustain. We argue that carbonate system closure and soil acid-base balance are necessary constraints on estimates of CDR at scale. Although the pH threshold for agronomically acceptable EW deployment will vary among soils and crops, a provisional pH limit of 7.5 provides a useful ceiling for model projections. As in agricultural liming, sustaining CDR at a stable pH requires balancing the alkalinity supply from weathering with acid production and drainage.

1 Introduction

For centuries, farmers have spread crushed rock on their fields to neutralize soil acidity and increase crop yields, a practice known as liming (Goulding, 2016; Winiwarter & Blum, 2008). But a central lesson from liming has been that more rock is not always better: high doses ("over-liming") can lower soil fertility and yields. Applied in excess, lime can raise pH high enough to cause nutrient deficiencies and raise the risk of disease (Adams, 1984; Fageria & Baligar, 2008; Lacey & Wilson, 2001; Levy et al., 2024; Parker & Walker, 1986; Walker et al., 2015). To ensure agricultural liming is sustainable over time, land managers must balance the addition of rock-derived alkalinity against the production of acidity in the soil, holding pH in a healthy range.

Enhanced weathering on croplands (EW) is essentially the same practice as liming — spreading cation-rich rock on managed lands — but with an additional goal. EW promises to improve soil health and crop

yields while also delivering globally significant amounts of carbon dioxide removal (CDR). However, tension between these goals is starting to emerge (Levy et al., 2024; Mao et al., 2026; Power et al., 2026). Most crops gain little from pH rising above neutral, and pushing pH too high (typically above 7.5 or 8) can cause adverse agronomic effects (Arrobas et al., 2023; Farhangi-Abriz et al., 2021; Farina et al., 1980; Leeper, 1934; Mulder & Gerretsen, 1952; Olego et al., 2021). In contrast, higher porewater pH favors greater bicarbonate concentrations and alkalinity export, potentially increasing CDR. This means the CDR a field can sustain may be limited by the pH levels its crops can tolerate.

Whether this agronomic constraint limits the scale of EW depends on the magnitude of CDR that can be sustained without excessive soil alkalinization. Regional and global "scoping models" have provided the principal quantitative basis for projections of gigaton-scale CDR from EW, shaping expectations of its potential for substantial climate mitigation (Beerling et al., 2020; Fuhrman et al., 2023; Gaucher et al., 2025; Strefler et al., 2018; Tu et al., 2026). These models — including integrated assessment models, technological diffusion models, and some geochemical models — simplify the processes governing mineral weathering and alkalinity export in order to evaluate EW potential at regional and global scales. However, most do not explicitly account for the pH response to EW, leaving it unclear the extent to which their projected CDR fluxes are compatible with agronomically acceptable soil conditions.

The agricultural liming literature offers an independent benchmark for these projections. Long-term liming studies have found that, to hold pH near neutral, cropland can accommodate alkalinity inputs equivalent to about 0.01–2.0 t ha^{-1} yr^{-1} of CDR (Bolton, 1977; Chambers & Garwood, 1998; Dolling & Porter, 1994; Gascho & Parker, 2001; Guo et al., 2010; Helyar et al., 1990; Holland et al., 2019; Moody & Aitken, 1997; Ridley et al., 1990; Tsao et al., 2025; Zhu et al., 2018). Expressed per hectare, most scoping model projections are several times higher (Figure 1). Liming research therefore suggests that the alkalinity inputs required to sustain these projected CDR fluxes would push pH well above neutral (Fageria & Baligar, 2008; Goulding, 2016). Yet, the only scoping model we are aware of that tracks pH, which we refer to as B25, has found that similarly high CDR fluxes can be sustained for decades on U.S. cropland while keeping pH near neutral (Beerling et al., 2020, 2025). This discrepancy raises a fundamental question: can croplands sustain the high CDR fluxes that scoping models project without alkalizing?

Here, we examine this question by evaluating the relationship between CDR and pH, focusing on the aqueous carbonate chemistry that connects them. We use B25 as a test case because it is the only scoping model that reports quantities needed to evaluate carbonate system closure and, ultimately, the potential for soil alkalization. When we close the carbonate system, a clear trade-off emerges: sustaining B25's CDR fluxes across the U.S. pushes pH above 8 nearly everywhere. If we instead enforce near-neutral pH, CDR decreases by more than 80 percent. This trade-off applies to any scoping model that projects high CDR fluxes, whether or not the model solves for pH. It is often obscured because soil processes that resist pH change do so by consuming alkalinity that could otherwise be exported as CDR, and when that alkalinity loss goes uncounted, high CDR can appear achievable with only modest changes in pH. As a result, we argue the high CDR fluxes projected by scoping models would likely trigger widespread soil alkalization, and future models should either revise those fluxes or show they keep pH in an agronomically safe range. More broadly, sustained alkalinity export in cropland EW is not

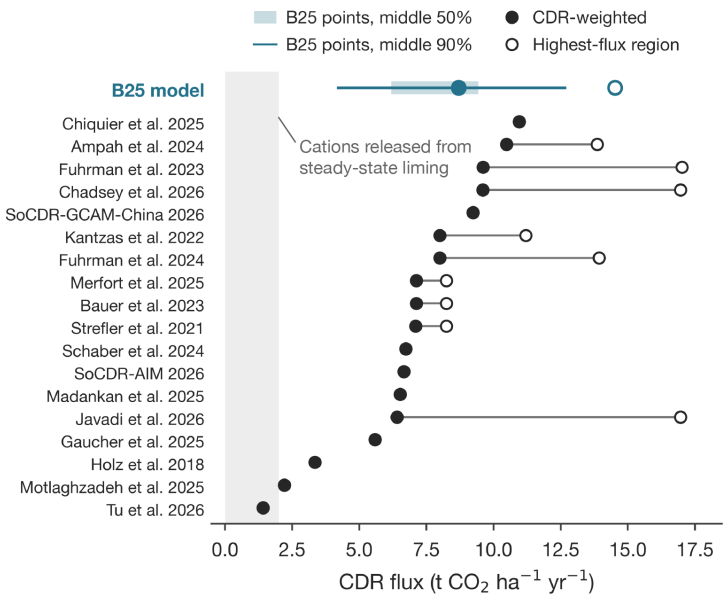


Figure 1: CDR fluxes from regional and global EW scoping models compared to the B25 model. Filled symbols refer to the CDR-weighted flux (using the highest EW-scenario of those presented), while open symbols refer to the geographic region with the highest modeled flux. SoCDR refers to the State of CDR report (3rd edition, Gidden et al., 2026). The gray bar denotes the CDR potential based on the cation flux from lime application studies that maintain a target pH. See supplementary text for more information on computing CDR fluxes from global scale estimates.

simply a question of mineral dissolution rates, but also the limits on soil inputs required to maintain agricultural productivity.

2 Balancing CDR and pH in buffered soils

For the sole purpose of maximizing CDR, a larger increase in pH is almost always better. At a given soil CO_2 partial pressure (pCO_2), the aqueous carbonate system relates pH to alkalinity such that raising one necessarily raises the other. The rise in pH determines how much more carbonate alkalinity the porewater can hold, and the CDR flux is roughly the product of the added alkalinity and the rate at which the porewater drains. For crops, however, an increase in pH is typically only favorable up to a point. Most crop yields peak in slightly acidic to neutral soils (pH ~6-7) and, above 7, soils are often referred to as alkaline. In addition to micronutrient deficiencies and increased disease risk (Fageria & Baligar, 2008; Lacey & Wilson, 2001; Paulitz & Schroeder, 2016), soil alkalization can lead to soil carbonate formation that limits phosphorus availability, restricts water movement, and makes it harder for farmers to manage the pH of their field (Penn & Camberato, 2019). Soil alkalization may also enhance the mobility of naturally occurring contaminants, including uranium due to carbonate complexation and selenium under alkaline, oxidizing conditions, potentially posing risks to groundwater used for drinking water (Fio et al., 1991; Jurgens et al., 2010).

How much the pH can rise above neutral before adverse effects set in, or before a land manager is

uncomfortable with the risk, will vary by crop, soil, and land management practice and norms; we return to this question later. Regardless of the pH threshold, EW deployments on croplands all face the same challenge: raising pH high enough to get meaningful levels of CDR, but not so high that it leads to reduced crop yields or other negative side effects. For simplicity, we discuss CDR based on the carbonate alkalinity exported from the soil (mostly as bicarbonate at the pH values considered here). However, we note that CDR is generally considered to be the share of alkalinity that is durably stored as dissolved inorganic carbon, typically in the ocean (Clarkson et al., 2024; Kanzaki et al., 2023).

In the near term, it may appear that achieving a high CDR flux at near-neutral pH is straightforward. Soils initially resist changes in pH through the neutralization of reserve acidity, which makes it possible to weather large amounts of rock without large increases in pH (Holden et al., 2024; Jessen et al., 2026; Maher et al., 2026; Nelson & Su, 2010; Rogers & Maher, 2026; Su et al., 2026). Empirical buffer curves and lime recommendations describe this behavior as a titration, relating a change in soil pH to the cumulative amount of acid or base added to the soil. However, at least initially, much of that base is neutralized by reserve acidity buffering rather than remaining in the porewater, which reduces its immediate export from the soil, and with it CDR.

Eventually, with continued EW, pH approaches a dynamic steady-state between acidity production due to soil respiration and fertilizer inputs, weathering-derived alkalinity inputs, and alkalinity loss and export. The buffer dampens both pH and CDR on the way to this steady state, but it does not set the CDR flux once it is reached. Instead, buffering determines how much rock must weather to reach a target pH, which is why liming recommendations call for larger doses in more strongly buffered soils (Supplementary Figure S1). At a fixed pH, CDR is limited by how much alkalinity porewater can carry at a given soil pCO_2. If instead the soil re-acidifies, some of the alkalinity consumed by buffering could be returned. That would shift some CDR later in time, but it would not raise the flux that can be sustained at a target pH.

Because pH buffering consumes alkalinity, feedstock weathering rates and CDR are different quantities: weathering provides a source of alkalinity, and CDR is the alkalinity that is ultimately exported. If weathering rates are the metric for CDR, buffered soils can appear to support a large CDR flux without alkalizing. However, if the pH response to alkalinity is smaller than the carbonate system predicts, then some alkalinity must have been consumed between weathering and export, and therefore did not contribute to CDR (Holden et al., 2024; Power et al., 2025; Steinwidder et al., 2025; Te Pas et al., 2025; Vienne et al., 2024, 2026). Consequently, in buffered soils, near-term weathering fluxes are not a reliable indicator of near-term CDR, nor of the CDR fluxes that can be sustained at a target pH (Holden et al., 2024; Kanzaki et al., 2025; Maher et al., 2026; Mao et al., 2026; Power et al., 2025; Su et al., 2026).

A limitation of nearly all scoping models is that they treat weathering rates as roughly equivalent to CDR, though in different ways. Most scoping models only quantify weathering — pH is not tracked and no buffering reactions consume alkalinity (Chiquier et al., 2025; Fuhrman et al., 2023; Gaucher et al., 2025; Ruan et al., 2026; Strefler et al., 2021). B25 is an important exception. By tracking pH and soil buffering, it is the only scoping model we are aware of in which the agronomic consequences of EW can be evaluated directly, representing an important advance (Beerling et al., 2020, 2025). Capturing

buffering in a scoping model, however, requires simplifications, and these affect the relationship between CDR and pH in B25. The model uses an empirical buffering curve adapted from Nelson & Su (2010) to dampen the pH response to EW. The curve sets pH but does not remove alkalinity from porewater, so the alkalinity that buffering would neutralize remains available to be exported as CDR. In other words, the buffer applies to pH, but not to CDR. B25 also drives the buffer relationship with porewater alkalinity concentrations, rather than cumulative net alkalinity added to the soil. This allows B25's porewater chemistry to approach steady state, as a real soil would, but its steady-state pH comes from the buffer curve rather than carbonate equilibrium with exported alkalinity and soil pCO_2. Together, these simplifications permit high CDR fluxes at near-neutral pH that can be sustained for decades.

Using the carbonate system quantities reported in B25 as an example, we now turn to the question of whether the high CDR fluxes pervasive in scoping models would cause soil alkalization. At a given temperature, aqueous carbonate equilibrium constrains the relationship among pH, alkalinity, and soil pCO_2. Unlike other scoping models, B25 simulates all three, allowing us to evaluate carbonate system closure using any two variables.

We use B25's alkalinity and soil pCO_2 to calculate the pH under carbonate system closure and compare to the model prediction in Figure 2a. In doing so, we treat B25's alkalinity as carbonate alkalinity, consistent with its use as the basis for quantifying CDR. B25 predicts a median pH of 7.11 under EW deployments where about 20–30 tonnes of basalt weather per hectare per year (Supplementary Figure S2), with only 4 percent of site-years above a pH of 8. In contrast, the pH calculated from carbonate equilibrium has a median of 8.5 with all site-years exceeding pH 8. Agricultural liming recommendations in the U.S. provide an independent comparison, indicating that the modeled pH rise in B25 could be achieved with only a one-time application of much less alkalinity than B25 adds each year (Supplementary Figure S3).

In theory, raising soil pCO_2 could support greater porewater alkalinity export while keeping pH near-neutral. However, reconciling B25's modeled alkalinity and pH distributions requires substantially higher soil pCO_2 than the model predicts (Figure 2b). Closing the carbonate system requires median soil pCO_2 to be 50,000 ppm — about 26 times higher than the model's median soil pCO_2 levels, and roughly two times greater than some of the highest values reported in the upper 20 cm of cropland soils (Lockhart et al., 2023; Saccardi et al., 2025; Yonemura et al., 2009; Zhang et al., 2023).

3 The trade-off between high CDR fluxes and neutral pH

The relationship between porewater pH and the alkalinity that leads to CDR is highly nonlinear. Because pH is on a logarithmic scale, the amount of alkalinity in porewater at a given soil pCO_2, and therefore CDR, rises roughly tenfold with each pH unit increase (Figure 3a). This relationship holds CDR relatively low at a pH of 7, which could present a strong incentive to push soils alkaline.

To quantify this constraint, we use B25's modeled pH and soil pCO_2 to calculate the alkalinity consistent

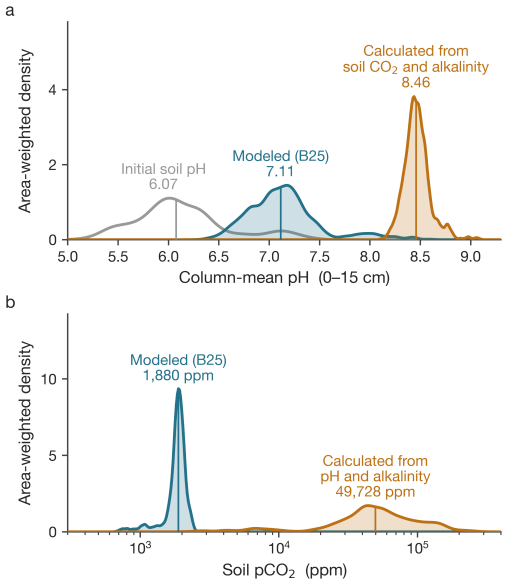


Figure 2: (a) Soil porewater pH in the initial soil (gray, no fill), modeled in B25 (blue), and calculated given B25's soil pCO_2 and alkalinity (orange). (b) Soil pCO_2 modeled in B25 (blue) compared to the pCO_2 required to close the carbonate system given the modeled pH and alkalinity (orange). Distributions use data from every year at each site, starting from the third year after rock application begins — after porewater pH has leveled out (see Supplementary Figure S2).

with carbonate system closure, then multiply by the modeled water infiltration rate to convert to CDR (Supplementary Figure S4). The pH values for B25 shown in Figure 3a are higher than they are in Figure 2a because Figure 3a shows the value at the base of the model's 15 cm profile, where alkalinity exits, rather than the column mean. Yet, even at this elevated pH, closing the carbonate system shifts CDR fluxes down from a median of 7.3 t ha^{-1} yr^{-1} to 1.0 t ha^{-1} yr^{-1}, with 90 percent of site-years below 2.3 t ha^{-1} yr^{-1} (Figure 3a). Other scoping models would likely face a similar constraint. Even for sites with high water infiltration (1 m yr^{-1}) and soil pCO_2 (15,000 ppm), both of which favor CDR, the steady-state carbonate-constrained CDR flux only reaches about 0.8 t ha^{-1} yr^{-1} at a pH of 7, and 2.8 t ha^{-1} yr^{-1} at pH 7.5 (dashed line in Figure 3a). The 4–12 t ha^{-1} yr^{-1} of CDR that many scoping models estimate lie well past that range, on the steep, alkaline end of the curve.

Figure 3b scales these fluxes up to U.S.-wide CDR. Closing the carbonate system lowers the annual CDR rate by 2070 by roughly a factor of 5, from 0.19 to 0.04 Gt yr^{-1}. These estimates assume that soil carbonate formation does not count as durable CDR due to the risk of reversal after EW applications end. If we count soil carbonate formation as CDR, all numbers shift higher but the relative differences are similar (Supplementary Figure S5). These estimates also ignore pH buffering from reserve acidity, which would further decrease near-term CDR fluxes.

Taken together, on most cropland it seems unlikely that EW can deliver both CDR fluxes above ~2 t ha^{-1} yr^{-1} and near-neutral pH. Recent work found that this applies globally. At a pH of 7.5 and soil pCO_2 of 10,000 ppm, Mayer et al. (2025) showed that most cropland can export no more than 1 t ha^{-1} yr^{-1} of CDR. That is not to say that this is a hard limit on agronomically sustainable CDR. But, in the context

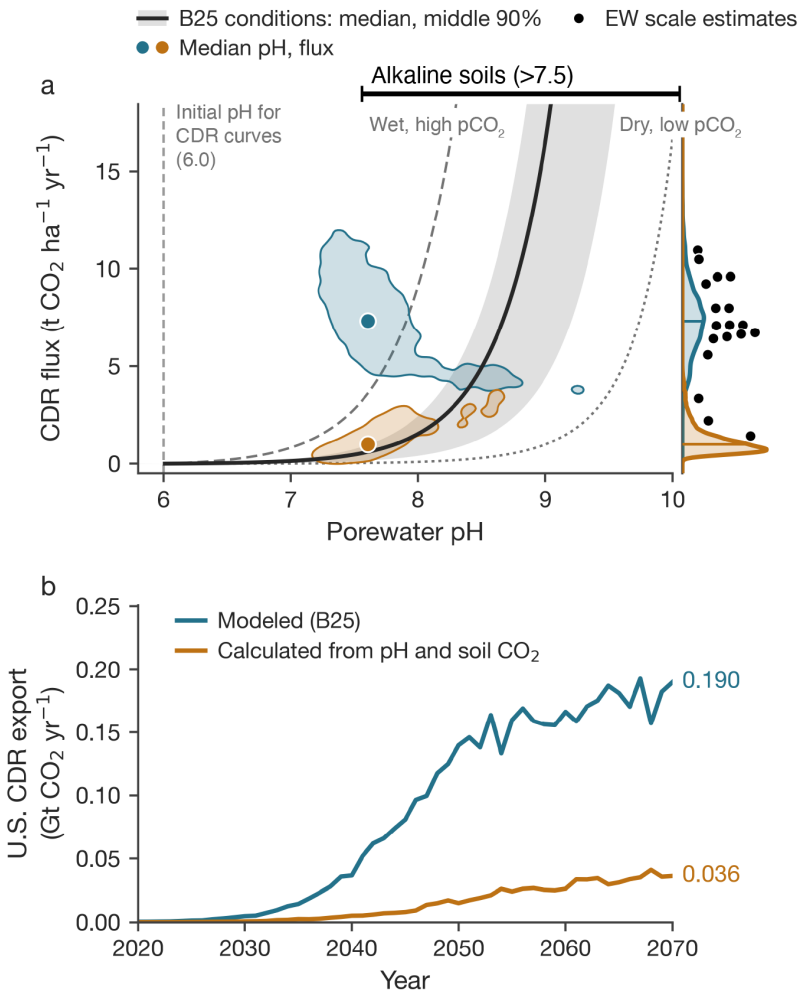


Figure 3: (a) CDR fluxes versus porewater pH. The blue contour and histogram denote B25's modeled results, whereas the orange contour and histogram close the carbonate system at the modeled pH. Points show median values. Curves show CDR-pH relationships for various infiltration rates and soil pCO_2 levels. The black curve denotes the median B25 site, and the ribbon the middle 90 percent. The dashed line (wet, high pCO_2) assumes 1 m yr^{-1} infiltration and 15,000 ppm soil pCO_2. The dotted line (dry, low pCO_2) assumes 0.1 m yr^{-1} infiltration and 1,500 ppm soil pCO_2. All curves assume an initial pH of 6.0. Black points refer to CDR-weighted fluxes from the scale estimates shown in Figure 1. (b) Annual CDR rates across the U.S. The blue curve refers to B25, and the orange curve shows CDR fluxes assuming the model's porewater pH and soil pCO_2, closing the carbonate system.

of our analysis, it puts CDR fluxes above 1–2 t ha^{-1} yr^{-1} in a complicated gray area. While those fluxes are achievable at neutral pH in some places, they seem likely to cause soil alkalization at scale. The consequences of such widespread alkalization deserve more scrutiny.

4 Implications of an agronomic ceiling on CDR

The steep nonlinear relationship between pH and alkalinity means that even small changes in pH matter — for a given soil pCO_2, raising pH by just a tenth of a unit could deliver roughly a quarter more CDR. The upper pH limit that crops can tolerate without adverse effects is not well established and likely depends on the crop, climate, and soil conditions. Nevertheless, assuming such a limit exists, two consequential questions follow: Can we raise the agronomic ceiling, and can we get close to it without surpassing it?

First, it may be possible to raise the agronomic ceiling on EW by mitigating some of the adverse effects of soil alkalization. A similar problem has been addressed in limed and naturally alkaline soils, but the known solutions tend to be expensive or risky to deploy at scale. For example, farmers could switch to more alkali-tolerant crops, such as wheat, though that could imply the loss of acid-tolerant crops, such as potatoes, at scale. Farmers could also use micronutrient-rich fertilizers (Cakmak, 2008; Kaiser et al., 2014), but that would require scaling additional agricultural inputs alongside the rock itself. Researchers could also develop more alkali-tolerant crop strains — an approach that has seen some promise adapting crops to naturally alkaline soils (Bavaresco et al., 2003; Waters et al., 2018), but one that would likely require large investments in research and development with no guarantee of success.

The second challenge involves optimizing CDR so that EW deployments approach the agronomic ceiling without surpassing it. Here, again, liming practices have historical precedent and learning to offer EW. Farmers often apply lime at a uniform rate across a field, and they sometimes decrease their lime dose so that the less acidic parts of a field are not over-limed. In many cases, this is acceptable because the pH range for optimal yields is larger than the pH variability of the field. But in cases where the target pH range is narrow, variable rate spreaders offer more precision. These systems dynamically adjust the lime spreading rate to meet the pH needs of a specific part of a field (Bönecke et al., 2021). In theory, that precision could help EW deployments push an entire field to a target pH without surpassing it. Accessing that precision at scale, however, would require much broader adoption of variable rate spreaders, which are currently a niche technology (McFadden et al., 2024).

5 Toward agronomically sustainable CDR estimates

The CDR projections put forth by many scoping models seem likely to imply widespread soil alkalization. How much that might limit EW at scale, however, remains an open question. Agronomically sustainable EW deployments — those that can maintain pH levels acceptable to crops and land managers — are not well defined, in part because deliberate soil alkalization is uncommon. Some studies on over-liming show that alkalization can limit plant uptake of boron, zinc, iron, and manganese (Arrobas et al., 2023; Leeper, 1934; Mulder & Gerretsen, 1952; Olego et al., 2021), cause aluminum toxicity (Farina et al., 1980), raise the

risk of diseases such as potato scab (Lacey & Wilson, 2001; Paulitz & Schroeder, 2016), and reduce yields (Fageria & Baligar, 2008; Sumner et al., 1978). Naturally alkaline soils face similar problems (Alloway, 2009; Cakmak et al., 1996; Hansen et al., 2004; Kaiser et al., 2014). But which of these effects appears, and at what pH, depends on the crop and the soil, and some crops could see no adverse effects at all (Holland et al., 2019, 2024; Pearson et al., 1975). Though, even if crop yields stay high as soils alkalize, farmers may be uncomfortable with the risk of pushing pH beyond familiar thresholds, or with the precipitation of soil carbonates that could hinder future pH management. There is a lot more work to do if we want to seriously consider CDR deployments that alkalize the soil.

The agronomic sustainability of EW has not been a major research focus, partly because it is not a near-term problem. Because most soils are buffered, they can absorb some years of alkalinity dosing before registering a large pH response (Jessen et al., 2026; Maher et al., 2026). It may take 5–10 years (or longer) before EW deployments approach critical agronomic thresholds that require adjustments. For this reason, integrated experimental and modeling approaches will play a major role in helping us connect near-term results to the long-term trade-offs between EW and agronomic outcomes.

If EW is expected to maintain near-neutral pH, then many of the CDR fluxes underpinning scoping model estimates are too high. Our analysis indicates that near-neutral pH conditions are rarely compatible with steady state CDR fluxes above 2 t ha^{-1} yr^{-1}, and often push CDR below 1 t ha^{-1} yr^{-1}. Liming and acidification studies support this result. They find that, to maintain a neutral, constant pH, calcium carbonate has to be consumed at a flux of about 0.01–2.2 t $CaCO_3$ ha^{-1} yr^{-1}, with higher fluxes supporting a higher target pH (Bolton, 1977; Chambers & Garwood, 1998; Dolling & Porter, 1994; Gascho & Parker, 2001; Guo et al., 2010; Helyar et al., 1990; Holland et al., 2019; Moody & Aitken, 1997; Ridley et al., 1990; Tsao et al., 2025; Zhu et al., 2018). That equates to a maximum CDR flux of about 2.0 t ha^{-1} yr^{-1} assuming a silicate feedstock (or half as much for a carbonate feedstock) and assuming that all dissolution is driven by carbonic acid. These steady state fluxes are consistent with many CDR estimates in the EW literature (Suhrhoff et al., 2026), but they are lower than some recent CDR issuances (Isometric, 2026; Puro.earth, 2025, 2026). Extrapolated out, the issuances with the highest CDR fluxes would likely overestimate the sustainable scale potential of EW.

The next generation of EW scoping models should account for agronomic sustainability, even while acceptable pH thresholds are uncertain. Until those limits are better constrained, we suggest a pH of 7.5 as a provisional upper bound. It is high enough that, in the U.S., most agricultural extensions do not publish the amount of lime required to get there, either because there are no further yield benefits or there is a greater risk of yield loss (see Kukla, 2026f for compiled extension recommendations). It is also low enough that some crop yields could be unaffected (Holland et al., 2019, 2024; Pearson et al., 1975). In the range between the dry, low pCO_2 and wet, high pCO_2 cases from Figure 3a, a pH of 7.5 constrains CDR to roughly 0.03–2.8 t ha^{-1} yr^{-1} (Mayer et al., 2025).

To make the pH response to CDR clear, we argue that scoping models should, at a minimum, close the carbonate system. We also strongly caution against using weathering rates, empirical or lab-derived, to calibrate these models without other inputs (Chiquier et al., 2025; Fuhrman et al., 2023; Gaucher et al., 2025; Ruan et al., 2026; Strefler et al., 2021; Tu et al., 2026). By themselves, weathering rates do not

offer any insight into the pH response, and high weathering rates that occur with a small pH response typically point to alkalinity being consumed rather than contributing to CDR.

The carbonate system is just one constraint on the relationship between EW, cropland pH, and agronomic sustainability. EW researchers should push toward a more complete picture of what agronomically sustainable CDR looks like from the ground up. That requires studying a broader suite of processes relevant to CDR and agriculture (Levy et al., 2024; Power et al., 2026), including reserve acidity buffering (Holden et al., 2024; Jessen et al., 2026), (micro)nutrient availability (Desmalles et al., 2025; Swoboda et al., 2022), the buildup of secondary minerals (Steinwidder et al., 2025; Vienne et al., 2026), interactions with soil organic matter (Buss et al., 2024; Sokol et al., 2024), and soil structure and hydrology (Anand et al., 2026; Dupla et al., 2024; Levy et al., 2024; Nelson & Ham, 2000). Empirical work on these fronts is underway, but we also need more experimentally informed modeling work to simulate longer time horizons that move beyond the soil acidity buffering regime and toward a new steady state. Following agricultural liming practices, a vision for sustainable EW requires framing it as a problem of acidity demand, rather than one of weathering rates and alkalinity supply. Without a clear vision for balancing alkalinity and acidity at steady state, EW may fail to deliver on its promise of both CDR and agronomic benefit.

Acknowledgements

We are grateful for feedback from Grayson Badgley and Chris Allen that improved the manuscript. Tyler Kukla thanks Raphael Hagen for software support. Tyler Kukla, Zach Perzan, and Freya Chay were supported in part by a grant to CarbonPlan from the Chan Zuckerberg Initiative DAF, an advised fund of Silicon Valley Community Foundation.

Conflict of interest

The authors declare no competing interests.

Data availability

All data presented in the manuscript is available on Zenodo under CC-BY license, including geochemical results (Kukla, 2026d), compiled U.S. lime recommendation data (Kukla, 2026f), and compiled scoping model CDR results (Kukla, 2026e). Code to reproduce our calculations and figures is available on GitHub under MIT license (Kukla, 2026a, 2026b, 2026c).

Supporting Information

S1 CDR fluxes from scoping models

For each scoping model study in Figure 1, we select the model projection with the most EW CDR in its peak year, and divide peak year CDR by the land area available for EW deployment. We use the model scenarios with the largest EW deployment per study because they allow us to analyze the agronomic implications of ambitious EW scale volumes. Figure 1 reports both the CDR-weighted flux (weighted by each region's contribution to total CDR) and the highest regional CDR flux. To compute CDR fluxes from regional or global rates, we use the model's own land area constraints where available (or the rock applied divided by the application rate). For studies that use REMIND-MAgPIE, we apply the regional EW cropland availability presented in the supplement of Strefler et al. (2021). Otherwise, we assume that EW is deployed uniformly on 50 percent of each region's 2015 cropland (Mehrabi et al., 2024), based on an estimate that roughly 50 percent of cropland is acidic enough to benefit from EW (Levy et al., 2024). For studies that model a single region, where the global cropland fraction limit may not apply, we assume that 100 percent of regional cropland is available for EW. See supplementary Table S1 and Table S2 for study-specific information about our CDR flux calculations.

S2 B25 simulations

Our analysis of the B25 results builds on published output (Kantzas, 2025) and model code (Beerling et al., 2025; Lomas & Kantzas, 2024). The published outputs report annual CDR and mean pH (with pH averaged over the 0–15 cm soil column) for each deployment location. Because our analysis uses additional model fields, we re-ran B25 and validated our results against the published annual CDR and mean pH data. The additional fields our analysis leverages are porewater alkalinity, time-varying soil pCO_2, water infiltration rate, and pH at the base of the column. The model reports alkalinity based on the charge balance of base cations and strong acid anions, which is assumed to approximate carbonate alkalinity when calculating CDR.

We ran the B25 code (Lomas & Kantzas, 2024) in Octave, the open source alternative to Matlab. We used the large language model Claude (Opus 4.8) to help adapt the code to Octave. We kept B25's chemistry, physics, and default parameters, and only changed what was needed to output the model's internal state at each of 31 depth nodes 100 times per year. All changes are documented as diffs against the original code and can be fully reconstructed in the code repository (Kukla, 2026b). We simulated all 221 soil-climate clusters deployed in B25's 1 Gt yr^{-1} basalt scenario, following the model's deployment schedule through 2070. As in B25, each cluster is run twice, once for each of two basalt mineralogies by source state. The results for each cluster are then averaged between the two mineralogies, weighted by the state-specific weights from Extended Data Figure 3a of Beerling et al. (2025). Our runs reproduce B25's published results at each point and year to within 0.03 percent of each point's cumulative CDR and 0.004 pH units. Full validation can be found in the code repository (Kukla, 2026b).

S3 Carbonate system equilibrium and closure

Following B25, porewater alkalinity is based on the ion charge budget:

$$\mathrm{Alk_{B25}} = \mathrm{Alk_{bg}} + 2[\mathrm{Ca^{2+}}] + 2[\mathrm{Mg^{2+}}] + [\mathrm{K^{+}}] + [\mathrm{Na^{+}}] \tag{S1}$$

where $\mathrm{Alk_{bg}}$ is the unamended, background porewater alkalinity, determined by inverting the empirical buffer curve (Nelson & Su, 2010) at the initial porewater pH, and then subtracting site-specific acidity inputs. $\mathrm{Alk_{bg}}$ is therefore treated as approximately the alkalinity required to maintain initial pH under steady state at the given buffering capacity. The cation terms are derived from basalt feedstock, whereas base cations in the background porewater are accounted for in $\mathrm{Alk_{bg}}$. $\mathrm{Alk_{B25}}$ is converted to pH at every timestep using an empirical buffer curve adopted from Nelson & Su (2010). This pH is then used to evaluate calcium carbonate saturation and drive mineral dissolution. CDR is calculated based on the export of base cations from the 15-cm soil column, and is recognized as an upper-bound potential estimate of carbonate alkalinity export (Beerling et al., 2025). The Nelson & Su (2010) buffer equation is a dose-response curve, not an equilibrium relationship, so it does not account for any alkalinity loss that the buffered pH response implies.

To close the carbonate system, we relate carbonate alkalinity to $\mathrm{pCO_2}$ and pH following

$$\mathrm{Alk_C} = K_H\, p\mathrm{CO_2} \left(\frac{K_1}{[\mathrm{H^{+}}]} + \frac{2K_1K_2}{[\mathrm{H^{+}}]^2} \right) + \frac{K_w}{[\mathrm{H^{+}}]} - [\mathrm{H^{+}}], \tag{S2}$$

using B25's constants ($\mathrm{p}K_H$ = 1.41, $\mathrm{p}K_1$ = 6.38, $\mathrm{p}K_2$ = 10.38, $\mathrm{p}K_w$ = 14.16). B25 sets the three carbonate system variables independently — $\mathrm{Alk_{B25}}$ from charge balance, pH from the empirical buffer, and soil $\mathrm{pCO_2}$ as a forced input — so they do not necessarily satisfy Equation S2. Equating $\mathrm{Alk_C}$ and $\mathrm{Alk_{B25}}$ assumes, following B25's CDR accounting, that base cations are charge balanced by dissolved inorganic carbon rather than other anions. We evaluate how close B25 is to closing Equation S2 in three steps. First, we use no-feedstock pH and $\mathrm{pCO_2}$ to calculate the background $\mathrm{Alk_C}$. This step ensures that we start with the carbonate system closed, so any departure is caused by how the relevant species evolve with feedstock weathering. This is also how B25 sets the initial porewater when buffering is turned off in the model. Second, we compute total carbonate alkalinity, $\mathrm{Alk_{tot}}$, at each timestep from background $\mathrm{Alk_C}$ plus the sum of base cations. This gives us how carbonate alkalinity evolves at each site and time due to weathering. Finally, we perform two checks for carbonate system closure. In the first, we assume B25's $\mathrm{pCO_2}$ and use $\mathrm{Alk_{tot}}$ to compute pH. In the second, we assume B25's pH and use $\mathrm{Alk_{tot}}$ to compute $\mathrm{pCO_2}$. In each case, the carbonate system is closed at every depth node and timestep, then averaged by year and depth and weighted by cluster area before plotting in Figure 2. We also repeat these calculations without closing the carbonate system in the initial porewater, which shifts the calculated pH and $\mathrm{pCO_2}$ higher because it increases the alkalinity of the initial porewater (Figure S6).

S4 CDR at the modeled pH in B25

Similar to B25, we quantify CDR based on the exported feedstock cation charge multiplied by the model's ocean re-equilibration efficiency, η. This approach implicitly assumes that the cation charge is entirely balanced by bicarbonate (HCO_3^-). Soil carbonate is excluded from the CDR calculation except in Supplementary Figure S5. To close the carbonate system at B25's pH, we use B25's pH and soil pCO_2 at the base of the 15 cm column and calculate the additional carbonate alkalinity that the draining porewater can carry. The additional carbonate alkalinity, ΔAlk_{max}, is treated as the equilibrium alkalinity at the modeled pH and soil pCO_2 minus the equilibrium alkalinity for the same soil and year with feedstock cations removed from the alkalinity budget (thus, imposing a lower, baseline pH). Because ΔAlk_{max} relates to pH nonlinearly, we calculate CDR by integrating $q \times \Delta Alk_{max}$ (where q is the porewater flux out the bottom of the column) at the model's native timestep, then integrate the model's cation charge flux, and re-scale B25's CDR based on the ratio of the two integrals. Taking the ratio ensures that any error introduced by the integration cancels.

S5 Supplementary Tables and Figures

Model	Dissolution	Alkalinity export	Cropland area limit	References	Notes
GCAM	Tuned for total dissolution in one year	Total export, no losses	None	(Ampah et al., 2024; Chadsey et al., 2026; Fuhrman et al., 2023, 2024; Javadi et al., 2026; Motlaghzadeh et al., 2025)	The same ERW geochemistry is used across all GCAM versions in the referenced papers.
REMIND-MAgPIE	Climate-dependent weathering rate of a constant 150 t ha^{-1} stock	Total export, no losses	Yes (humid and temperate treated separately)	(Bauer et al., 2023; Harris et al., 2026; Merfort et al., 2025; Strefler et al., 2021)	
C-ROADS + En-ROADS	NA	Total export, no losses	None	(Holz et al., 2018)	ERW is calculated from a global maximum capacity and a time-variable deployment percent.
GET-ACC2	About 13 percent of a fixed 150 t ha^{-1} basalt stock weathers per year	Total export, no losses	Yes (7.8 Mkm^2)	(Gaucher et al., 2025)	Inorganic and organic CDR are reported for ERW; we refer to just the inorganic results for consistency across models.
EPPA	Tuned for total dissolution in one year; fixed 20 t ha^{-1} yr^{-1} basalt application flux	Total export, no losses	No clear limit; required area can be computed from the fixed application flux of 20 t ha^{-1} yr^{-1}	(Chiquier et al., 2025)	
SCORE	NA	Total export, no losses	None	(Schaber et al., 2024)	ERW is calculated from a global maximum annual and cumulative capacity; capacity grows linearly from zero.
Tu et al. 2026	Climate-dependent weathering rate adjusted from a reference CDR flux of 1.5 t ha^{-1} yr^{-1}	Total export, no losses	Yes (50% or 75% of global cropland)	(Tu et al., 2026)	Feedstock dissolution is not explicitly modeled, but the model implicitly assumes 10 t ha^{-1} of olivine application.
Kantzas et al. 2022 (UK)	Kinetic dissolution of a basalt grain-size distribution in a 1-D soil profile, driven by soil climate, hydrology and pH	Alkalinity exported from the soil profile, with ocean re-equilibration losses; soil carbonate formation also counted	Yes (UK arable cropland; treated area grows with each basalt-supply scenario)	(Kantzas et al., 2022)	Uses B25 model. We report net CDR rather than gross.
Madankan et al. 2025 (UK)	Not modeled; per-cell CDR from Kantzas et al. (2022) is scaled by the rock each quarry supplies	As in Kantzas et al. (2022)	Yes (GB cropland; treated area is rock supplied at 40 t ha^{-1})	(Madankan et al., 2025)	Allocates quarry rock to cropland; CDR is net of extraction, grinding, transport and spreading emissions.

Table S1: Enhanced weathering representations in the IAMs and other scoping models of Figure 1. “NA” indicates feedstock dissolution is not modeled. Figure 1 also includes AIM 3.0 and GCAM-China from State of CDR (3rd edition, Gidden et al., 2026), and a preprint (Harris et al., 2026) reports ERW from WITCH, IMAGE and MESSAGE, but we did not find thorough descriptions of the ERW modules in those model versions.

Reference	Model	Scenario	Peak year	Max ERW CDR (Gt CO_2 yr^{-1})	CDR-weighted flux (t CO_2 ha^{-1} yr^{-1})	Highest-region flux (t CO_2 ha^{-1} yr^{-1})	Area basis
Chiquier et al. (2025)	EPPA	CDR Portfolio	2070	8.14	10.96	10.96	50% of world cropland
Ampah et al. (2024)	GCAM-TJU	HIGH	2050	2.15	10.48	13.86	50% of cropland, 11 GCAM regions
Fuhrman et al. (2023)	GCAM-CDR	exe_lowCCS1p5	2100	4.65	9.61	17.02	50% of cropland, 32 GCAM regions
Chadsey et al. (2026)	GCAM 7.4	Full Trade no biochar	2085	4.63	9.60	16.96	50% of cropland, 32 GCAM regions
SoCDR-GCAM-China 2026	GCAM China CDR v7	Highest Ambition	2050	1.24	9.24	9.24	100% of China cropland
Kantzas et al. (2022)	Kantzas-UK	S3, 2060–2070 mean	2065	0.0329	8.00	11.20	treated area, 3,234 grid cells, 4.18 Mha
Fuhrman et al. (2024)	GCAM 6.0	gcam-1p5	2100	2.88	8.00	13.93	50% of cropland, 32 GCAM regions
Merfort et al. (2025)	REMIND-MAGPIE	SepMark_12	2060	4.79	7.12	8.24	REMIND ERW cropland, 12 REMIND regions
Bauer et al. (2023)	REMIND	overshoot3_Budg600-fullOvershoot	2090	4.96	7.12	8.24	REMIND ERW cropland, 12 REMIND regions
Strefler et al. (2021)	REMIND-MAgPIE	C_SSP2-900-EW-only-RefAff-Const2045	2045	4.77	7.10	8.24	REMIND ERW cropland, 12 REMIND regions
Schaber et al. (2024)	SCORE	bet_1path_avg_NETs_T15_loMAC_optNETs	2100	5.00	6.73	6.73	50% of world cropland
SoCDR-AIM 2026	AIM 3.0	Delayed Ambition	2100	4.95	6.66	6.66	50% of world cropland
Madankan et al. (2025)	Madankan-UK-quarry	S3.a	2060	0.0273	6.52	6.52	treated area, rock ÷ 40 t ha^{-1}, 4.19 Mha
Javadi et al. (2026)	GCAM-USA	HCDR	2040	0.328	6.41	16.96	50% of cropland, 49 U.S. states
Gaucher et al. (2025)	GET-ACC2	1.5°C with high overshoot / EW on CL	2090	4.42	5.59	5.59	stated area, 7.9 Mkm^2
Holz et al. (2018)	C-ROADS	C-ROADS allCDR	2100	2.49	3.35	3.35	50% of world cropland
Motlaghzadeh et al. (2025)	GCAM-CDR	EPC1.5Q_NoBioImp_LimDAC	2085	0.0880	2.21	2.21	100% of Canada cropland
Tu et al. (2026)	Tu-diffusion	Scenario3	2067	1.05	1.42	1.42	50% of world cropland

Table S2: ERW carbon dioxide removal (CDR) in the peak year of the highest-ERW scenario of each study in Figure 1. Fluxes are regional CDR divided by area; the CDR-weighted flux is their CDR-weighted mean and the highest-region flux is the regional maximum. Area is 50 percent of each model region's 2015 cropland (Mehrabi et al., 2024) unless the study states its treated area. Models that report one country as a single region use all of its cropland, and studies using REMIND are computed based on REMIND's regional cropland (Strefler et al., 2021). Gridded fluxes are decade means, dated at the decade's midpoint. Where a study gives an application rate, its treated area is rock applied divided by that rate. State of CDR, which reports ERW only for 2035, 2050 and 2100, is represented by its global and its national model with the most ERW CDR (Gidden et al., 2026).

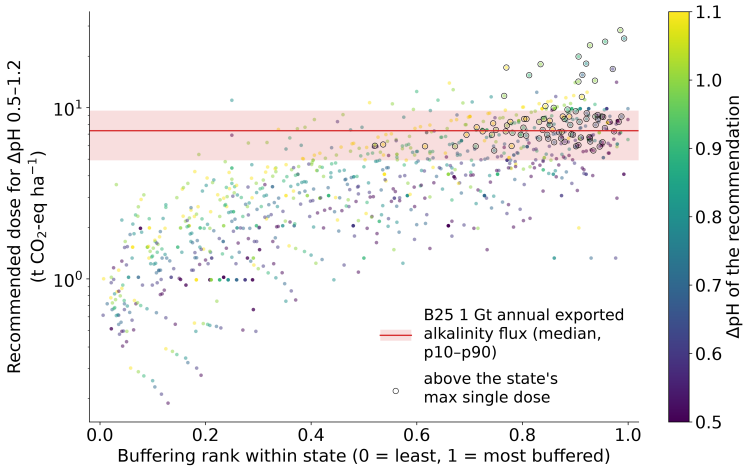


Figure S1: U.S. lime recommendations compared to the normalized buffering strength of the soil. Lime recommendations are expressed in units of CDR potential for simplicity. The red band shows the p10–p90 range of CDR fluxes from the B25 model, and the red line shows the median (Beerling et al., 2025). More strongly buffered soils require a larger lime dose to achieve the same pH increase.

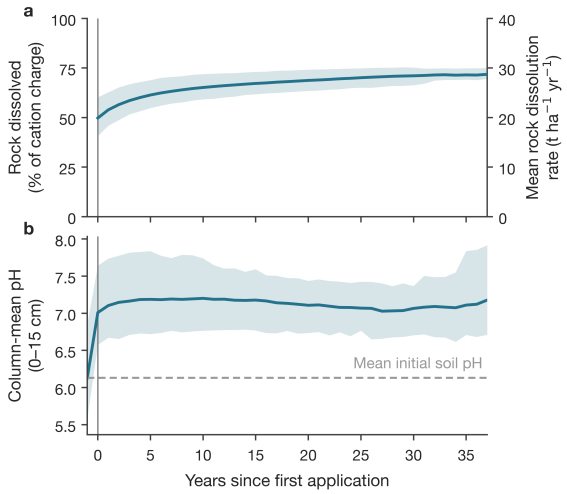


Figure S2: (a) Cumulative feedstock dissolution fraction and (b) column-mean porewater pH in Beerling et al. (2025) over time. Lines refer to the area-weighted mean, while ribbons span the 10th–90th percentile range. Feedstock dissolution is relative to 40 tonnes of basalt spread per hectare annually. Nearly all of the pH increase occurs in year 1 because the pH buffering effect is static through time.

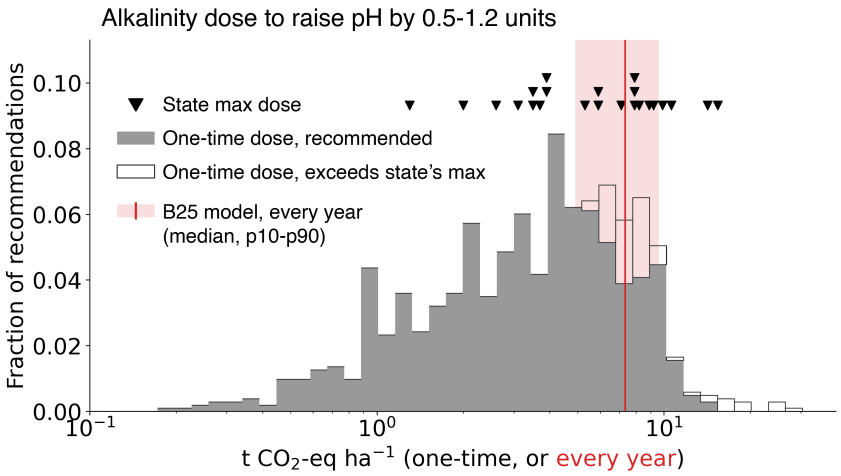


Figure S3: The one-time alkalinity dose required to raise soil pH by 0.5-1.2 units according to U.S. state lime recommendations (gray and transparent bars). These one-time doses are mostly below the annual alkalinity dose modeled in B25 to achieve the same pH response. To prevent soil alkalization, some states suggest maximum one-time doses (black triangles). Lime recommendations that exceed a state's own max dose are shown as transparent bars.

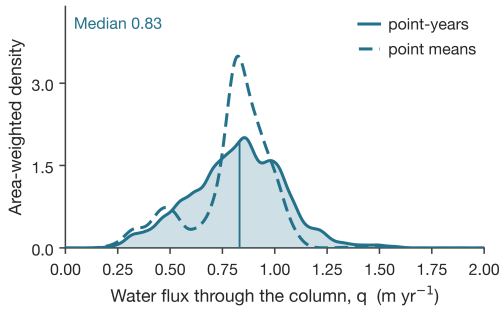


Figure S4: Water infiltration rates for U.S. sites in Beerling et al. (2025). Filled distribution spans all site-years. Dashed line distribution refers to time-means.

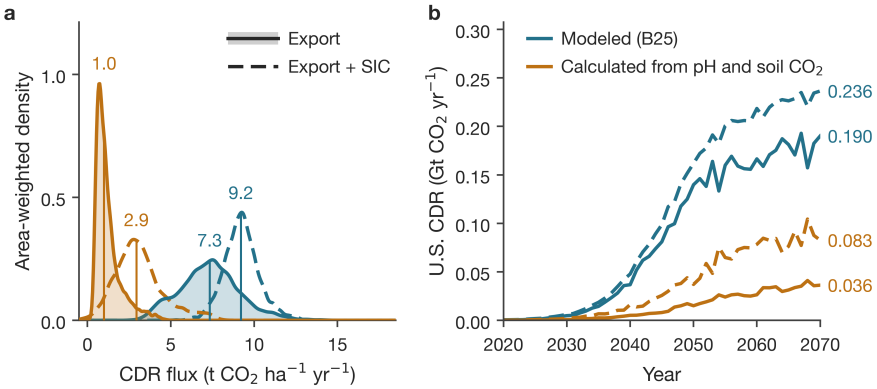


Figure S5: (a) CDR fluxes for B25 and carbonate equilibrium-corrected for two CDR definitions. Alkalinity export is shown with solid lines, and export plus carbon taken up by soil carbonate (SIC) is shown in dashed lines. (b) U.S.-wide CDR rate over time for the same CDR definitions. Accounting for SIC raises CDR, but the difference between B25 and the carbonate system constrained values remains similar.

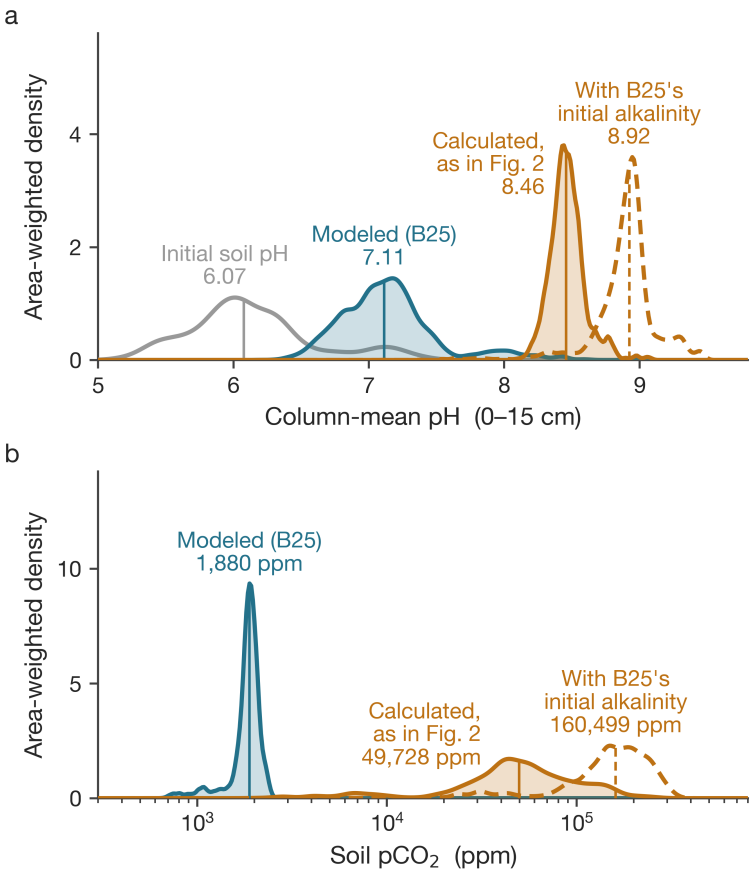


Figure S6: As in Figure 2 of the main text, but with pH and soil pCO_2 re-calculated assuming the initial porewater alkalinity concentration in the orange dashed lines (instead of reducing initial porewater alkalinity to achieve carbonate system closure). Accounting for excess alkalinity in the initial porewater pushes median pH up to 8.9 and median soil pCO_2 up to 160,500 ppm.

References

Adams, F. (1984). Crop Response to Lime in the Southern United States. In F. Adams (Ed.), *Agronomy Monographs* (1st ed., Vol. 12, pp. 211–265). Wiley. https://doi.org/10.2134/agronmonogr12.2ed.c5

Alloway, B. J. (2009). Soil factors associated with zinc deficiency in crops and humans. *Environmental Geochemistry and Health*, *31*(5), 537–548. https://doi.org/10.1007/s10653-009-9255-4

Ampah, J. D., Jin, C., Liu, H., Yao, M., Afrane, S., Adun, H., et al. (2024). Deployment expectations of multi-gigatonne scale carbon removal could have adverse impacts on Asia's energy-water-land nexus. *Nature Communications*, *15*(1), 6342. https://doi.org/10.1038/s41467-024-50594-5

Anand, S. K., Bertagni, M., Aburto, F., & Calabrese, S. (2026). Soil Structure and Mixing Controls on Water-Rock Contact: Implications for Enhanced Weathering. *Water Resources Research*, *62*(2), e2025WR041479. https://doi.org/10.1029/2025WR041479

Arrobas, M., Raimundo, S., Conceição, N., Moutinho-Pereira, J., Correia, C. M., & Rodrigues, M. Â. (2023). On Sandy, Boron-Poor Soils, Liming Induced Severe Boron Deficiency and Drastically Reduced the Dry Matter Yield of Young Olive Trees. *Plants*, *12*(24), 4161. https://doi.org/10.3390/plants12244161

Bauer, N., Keller, D. P., Garbe, J., Karstens, K., Piontek, F., Von Bloh, W., et al. (2023). Exploring risks and benefits of overshooting a 1.5 °C carbon budget over space and time. *Environmental Research Letters*, *18*(5), 054015. https://doi.org/10.1088/1748-9326/accd83

Bavaresco, L., Giachino, E., & Pezzutto, S. (2003). Grapevine Rootstock Effects on Lime-Induced Chlorosis, Nutrient Uptake, and Source–Sink Relationships. *Journal of Plant Nutrition*, *26*(7), 1451–1465. https://doi.org/10.1081/PLN-120021054

Beerling, D. J., Kantzas, E. P., Lomas, M. R., Wade, P., Eufrasio, R. M., Renforth, P., et al. (2020). Potential for large-scale CO2 removal via enhanced rock weathering with croplands. *Nature*, *583*(7815), 242–248. https://doi.org/10.1038/s41586-020-2448-9

Beerling, D. J., Kantzas, E. P., Lomas, M. R., Taylor, L. L., Zhang, S., Kanzaki, Y., et al. (2025). Transforming US agriculture for carbon removal with enhanced weathering. *Nature*. https://doi.org/10.1038/s41586-024-08429-2

Bolton, J. (1977). Changes in soil pH and exchangeable calcium in two liming experiments on contrasting soils over 12 years. *The Journal of Agricultural Science*, *89*(1), 81–86. https://doi.org/10.1017/S0021859600027210

Bönecke, E., Meyer, S., Vogel, S., Schröter, I., Gebbers, R., Kling, C., et al. (2021). Guidelines for precise lime management based on high-resolution soil pH, texture and SOM maps generated from proximal soil sensing data. *Precision Agriculture*, *22*(2), 493–523. https://doi.org/10.1007/s11119-020-09766-8

Buss, W., Hasemer, H., Sokol, N. W., Rohling, E. J., & Borevitz, J. (2024). Applying minerals to soil to draw down atmospheric carbon dioxide through synergistic organic and inorganic pathways. *Communications Earth & Environment*, *5*(1), 602. https://doi.org/10.1038/s43247-024-01771-3

Cakmak, I. (2008). Enrichment of cereal grains with zinc: Agronomic or genetic biofortification? *Plant and Soil*, *302*(1-2), 1–17. https://doi.org/10.1007/s11104-007-9466-3

Cakmak, I., Yilmaz, A., Kalayci, M., Ekiz, H., Torun, B., Erenoğlu, B., & Braun, H. J. (1996). Zinc deficiency as a critical problem in wheat production in Central Anatolia. *Plant and Soil*, *180*(2), 165–172. https:

//doi.org/10.1007/BF00015299

Chadsey, R., Harris, C., Diaoglou, V., Pratama, Y., Lamb, W. F., Rhalem, O., et al. (2026). Carbon dioxide removal consistent with climate pledges: A multi-model assessment of regional potential. *Environmental Science: Advances*. https://doi.org/10.1039/D6VA00109B

Chambers, B. J., & Garwood, T. W. D. (1998). Lime loss rates from arable and grassland soils. *The Journal of Agricultural Science*, *131*(4), 455–464. https://doi.org/10.1017/S0021859698005954

Chiquier, S., Gurgel, A., Morris, J., Chen, Y.-H. H., & Paltsev, S. (2025). Integrated assessment of carbon dioxide removal portfolios: Land, energy, and economic trade-offs for climate policy. *Environmental Research Letters*, *20*(2), 024002. https://doi.org/10.1088/1748-9326/ada4c0

Clarkson, M. O., Larkin, C. S., Swoboda, P., Reershemius, T., Suhrhoff, T. J., Maesano, C. N., & Campbell, J. S. (2024). A review of measurement for quantification of carbon dioxide removal by enhanced weathering in soil. *Frontiers in Climate*, *6*, 1345224. https://doi.org/10.3389/fclim.2024.1345224

Desmalles, C., Jordan-Meille, L., Hernandez, J., Thomas, C. L., Dunham, S., Deng, F., et al. (2025). Impact of Basalt Rock Powder on Ryegrass Growth and Nutrition on Sandy and Loamy Acid Soils. *Agronomy*.

Dolling, P., & Porter, W. (1994). Acidification rates in the central wheatbelt of Western Australia. 1. On a deep yellow sand. *Australian Journal of Experimental Agriculture*, *34*(8), 1155–1164. https://doi.org/10.1071/EA9941155

Dupla, X., Claustre, R., Bonvin, E., Graf, I., Le Bayon, R.-C., & Grand, S. (2024). Let the dust settle: Impact of enhanced rock weathering on soil biological, physical, and geochemical fertility. *Science of The Total Environment*, *954*, 176297. https://doi.org/10.1016/j.scitotenv.2024.176297

Fageria, N. K., & Baligar, V. C. (2008). Chapter 7 Ameliorating Soil Acidity of Tropical Oxisols by Liming For Sustainable Crop Production. In *Advances in Agronomy* (Vol. 99, pp. 345–399). Elsevier. https://doi.org/10.1016/S0065-2113(08)00407-0

Farhangi-Abriz, S., Torabian, S., Qin, R., Noulas, C., Lu, Y., & Gao, S. (2021). Biochar effects on yield of cereal and legume crops using meta-analysis. *Science of The Total Environment*, *775*, 145869. https://doi.org/10.1016/j.scitotenv.2021.145869

Farina, M. P. W., Sumner, M. E., Plank, C. O., & Letzsch, W. S. (1980). Aluminum toxicity in corn at near neutral soil pH levels. *Journal of Plant Nutrition*, *2*(6), 683–697. https://doi.org/10.1080/01904168009362807

Fio, J. L., Fujii, R., & Deverel, S. J. (1991). Selenium Mobility and Distribution in Irrigated and Nonirrigated Alluvial Soils. *Soil Science Society of America Journal*, *55*(5), 1313–1320. https://doi.org/10.2136/sssaj1991.03615995005500050020x

Fuhrman, J., Bergero, C., Weber, M., Monteith, S., Wang, F. M., Clarens, A. F., et al. (2023). Diverse carbon dioxide removal approaches could reduce impacts on the energy–water–land system. *Nature Climate Change*, *13*(4), 341–350. https://doi.org/10.1038/s41558-023-01604-9

Fuhrman, J., Speizer, S., O'Rourke, P., Peters, G. P., McJeon, H., Monteith, S., et al. (2024). Ambitious efforts on residual emissions can reduce CO_2 removal and lower peak temperatures in a net-zero future. *Environmental Research Letters*, *19*(6), 064012. https://doi.org/10.1088/1748-9326/ad456d

Gascho, G. J., & Parker, M. B. (2001). Long-Term Liming Effects on Coastal Plain Soils and Crops. *Agronomy Journal*, *93*(6), 1305–1315. https://doi.org/10.2134/agronj2001.1305

Gaucher, Y., Tanaka, K., Johansson, D. J. A., Goll, D. S., & Ciais, P. (2025). Leveraging ecosystems responses

to enhanced rock weathering in mitigation scenarios. *Nature Communications*, *16*(1), 3021. https://doi.org/10.1038/s41467-025-58284-6

Gidden, M. J., Portugal-Pereira, J., Apeaning, R., Bergero, C., Daioglou, V., Drouet, L., et al. (2026). Chapter 8: Paris-consistent CDR scenarios. In M. R. Edwards (Ed.), *The State of Carbon Dioxide Removal* (3rd ed.). Retrieved from https://www.stateofcdr.org/report/3rd-edition

Goulding, K. W. T. (2016). Soil acidification and the importance of liming agricultural soils with particular reference to the United Kingdom. *Soil Use and Management*, *32*(3), 390–399. https://doi.org/10.1111/sum.12270

Guo, J. H., Liu, X. J., Zhang, Y., Shen, J. L., Han, W. X., Zhang, W. F., et al. (2010). Significant Acidification in Major Chinese Croplands. *Science*, *327*(5968), 1008–1010. https://doi.org/10.1126/science.1182570

Hansen, N. C., Jolley, V. D., Naeve, S. L., & Goos, R. J. (2004). Iron deficiency of soybean in the North Central U.S. And associated soil properties. *Soil Science and Plant Nutrition*, *50*(7), 983–987. https://doi.org/10.1080/00380768.2004.10408564

Harris, C., Daioglou, V., Tagomori, I., Rhalem, O., Doelman, J., Fuhrman, J., et al. (2026, June). Carbon Dioxide Removal Supply Curves: A Multi-Model Assessment. EarthArXiv. https://doi.org/10.31223/X5C19K

Helyar, K., Cregan, P., & Godyn, D. (1990). Soil acidity in New-South-Wales - Current pH values and estimates of acidification rates. *Australian Journal of Soil Research*, *28*(4), 523–537. https://doi.org/10.1071/SR9900523

Holden, F. J., Davies, K., Bird, M. I., Hume, R., Green, H., Beerling, D. J., & Nelson, P. N. (2024). In-field carbon dioxide removal via weathering of crushed basalt applied to acidic tropical agricultural soil. *Science of The Total Environment*, *955*, 176568. https://doi.org/10.1016/j.scitotenv.2024.176568

Holland, J. E., White, P. J., Glendining, M. J., Goulding, K. W. T., & McGrath, S. P. (2019). Yield responses of arable crops to liming – An evaluation of relationships between yields and soil pH from a long-term liming experiment. *European Journal of Agronomy*, *105*, 176–188. https://doi.org/10.1016/j.eja.2019.02.016

Holland, J. E., White, R., Haefele, S. M., Goulding, K. W. T., McGrath, S. P., & Glendining, M. J. (2024). Long-term effects of lime and phosphorus application on soil extractable (Olsen) phosphorus differ between two arable UK soils. *Soil Use and Management*, *40*(4), e13160. https://doi.org/10.1111/sum.13160

Holz, C., Siegel, L. S., Johnston, E., Jones, A. P., & Sterman, J. (2018). Ratcheting ambition to limit warming to 1.5 °C – trade-offs between emission reductions and carbon dioxide removal. *Environmental Research Letters*, *13*(6), 064028. https://doi.org/10.1088/1748-9326/aac0c1

Isometric. (2026, April). Project Cajueiro (Mombak). Isometric Registry. Retrieved from https://registry.isometric.com/project/prj_1JZ0ZD3JN1S0SHW9

Javadi, P., O'Rourke, P., Fuhrman, J., Loughlin, D. H., Doney, S. C., Shobe, W., et al. (2026). Large-Scale Carbon Removal Will Create Public Health, Economic, and Climate Trade-Offs. *Environmental Science & Technology*, *60*(24), 17192–17205. https://doi.org/10.1021/acs.est.5c17950

Jessen, S., Jakobsen, R., Looms, M., Ambus, P., & Postma, D. (2026). Subsoil acidity causes long delays in inorganic carbon sequestration by Enhanced Weathering. arXiv. https://doi.org/10.48550/arXiv.2607.01835

Jurgens, B. C., Fram, M. S., Belitz, K., Burow, K. R., & Landon, M. K. (2010). Effects of Groundwater

Development on Uranium: Central Valley, California, USA. *Groundwater*, *48*(6), 913–928. https://doi.org/10.1111/j.1745-6584.2009.00635.x

Kaiser, D. E., Lamb, J. A., Bloom, P. R., & Hernandez, J. A. (2014). Comparison of Field Management Strategies for Preventing Iron Deficiency Chlorosis in Soybean. *Agronomy Journal*, *106*(6), 1963–1974. https://doi.org/10.2134/agronj13.0296

Kantzas, E. (2025, January). US EW modelling outputs (Beerling et al. 2025, nature). Zenodo. https://doi.org/10.5281/zenodo.14755424

Kantzas, E. P., Val Martin, M., Lomas, M. R., Eufrasio, R. M., Renforth, P., Lewis, A. L., et al. (2022). Substantial carbon drawdown potential from enhanced rock weathering in the United Kingdom. *Nature Geoscience*, *15*(5), 382–389. https://doi.org/10.1038/s41561-022-00925-2

Kanzaki, Y., Planavsky, N. J., & Reinhard, C. T. (2023). New estimates of the storage permanence and ocean co-benefits of enhanced rock weathering. *PNAS Nexus*, *2*(4), pgad059. https://doi.org/10.1093/pnasnexus/pgad059

Kanzaki, Y., Planavsky, N. J., Zhang, S., Jordan, J., Suhrhoff, T. J., & Reinhard, C. T. (2025). Soil cation storage is a key control on the carbon removal dynamics of enhanced weathering. *Environmental Research Letters*, *20*(7), 074055. https://doi.org/10.1088/1748-9326/ade0d5

Kukla, T. (2026a). b25-analysis: Post-process and analyze B25 enhanced weathering model results. GitHub. Retrieved from https://github.com/carbonplan/b25-analysis

Kukla, T. (2026b). b25-model-extension: Re-running the Beerling et al. (2025) weathering model in Octave. CarbonPlan. Retrieved from https://github.com/carbonplan/b25-model-extension

Kukla, T. (2026c). Lime-rec-synthesis: Harmonized US liming recommendations, CCE dose vs. pH response. CarbonPlan. Retrieved from https://github.com/carbonplan/lime-rec-synthesis

Kukla, T. (2026d, November). B25 model rerun results. Zenodo. https://doi.org/10.5281/zenodo.24389385

Kukla, T. (2026e, November). Enhanced weathering scoping model synthesis. Zenodo. https://doi.org/10.5281/zenodo.24387133

Kukla, T. (2026f, November). Liming recommendation data. Zenodo. https://doi.org/10.5281/zenodo.24117712

Lacey, M. J., & Wilson, C. R. (2001). Relationship of Common Scab Incidence of Potatoes Grown in Tasmanian Ferrosol Soils with pH, Exchangeable Cations and other Chemical Properties of those Soils. *Journal of Phytopathology*, *149*(11-12), 679–683. https://doi.org/10.1046/j.1439-0434.2001.00693.x

Leeper, G. W. (1934). Relationship of Soils to Manganese Deficiency of Plants. *Nature*, *134*(3399), 972–973. https://doi.org/10.1038/134972c0

Levy, C. R., Almaraz, M., Beerling, D. J., Raymond, P., Reinhard, C. T., Suhrhoff, T. J., & Taylor, L. (2024). Enhanced Rock Weathering for Carbon Removal–Monitoring and Mitigating Potential Environmental Impacts on Agricultural Land. *Environmental Science & Technology*, *58*(39), 17215–17226. https://doi.org/10.1021/acs.est.4c02368

Lockhart, S. R. A., Keller, C. K., Evans, R. D., Carpenter-Boggs, L. A., & Huggins, D. R. (2023). Soil CO2 in organic and no-till agroecosystems. *Agriculture, Ecosystems & Environment*, *349*, 108442. https://doi.org/10.1016/j.agee.2023.108442

Lomas, M., & Kantzas, E. (2024, April). US soil profile EW code. Zenodo. https://doi.org/10.5281/zenodo.

10940280

Madankan, M., Kantzas, E. P., Espinosa, R. M. E., Vetter, S. H., Koh, L., Smith, P., et al. (2025). Larger rock extraction sites could improve the efficiency of enhanced rock weathering in the United Kingdom. *Communications Earth & Environment*, *6*(1), 666. https://doi.org/10.1038/s43247-025-02656-9

Maher, K., Rogers, B., Perzan, Z., & Kukla, T. (2026). Surface Proton Reservoirs Constrain Alkalinity Export from Enhanced Weathering. *Environmental Science & Technology*. https://doi.org/10.1021/acs.est.6c03236

Mao, J., Hao, Y., Sholl, D. S., Gu, X., Wang, Y., Stack, A. G., et al. (2026). Enhanced rock weathering for sustainable carbon capture: Advances, challenges, and future prospects in terrestrial ecosystems. *Reviews in Environmental Science and Bio/Technology*, *25*(4), 46. https://doi.org/10.1007/s11157-026-09793-3

Mayer, K. U., Bea, S. A., Su, D., Soong, J., Mills, J., & Benner, S. G. (2025, December). Carrying capacity as constraint for maximum efficient CDR in agricultural soils. In Review. https://doi.org/10.21203/rs.3.rs-7811095/v1

McFadden, J., Erickson, B., Lowenberg-DeBoer, J., & Milics, G. (2024). Global Adoption of Precision Agriculture: An Update on Trends and Emerging Technologies.

Mehrabi, Z., Tong, K., Fortin, J., Stanimirova, R., Friedl, M., & Ramankutty, N. (2024, August). Global agricultural lands in the year 2015. ESSD – Land/Land Cover and Land Use. https://doi.org/10.5194/essd-2024-279

Merfort, A., Strefler, J., Abrahão, G., Bauer, N., Dorndorf, T., Kriegler, E., et al. (2025). Separating CO2 emission from removal targets comes with limited cost impacts. *Nature Communications*, *16*(1), 5298. https://doi.org/10.1038/s41467-025-60606-7

Moody, P. W., & Aitken, R. L. (1997). Soil acidification under some tropical agricultural systems. 1. Rates of acidification and contributing factors. *Australian Journal of Soil Research*, *35*(1), 163–174. https://doi.org/10.1071/S96069

Motlaghzadeh, K., Craik, N., Moreno-Cruz, J., Schweizer, V., Fuhrman, J., & Hipel, K. W. (2025). Applying equity principles leads to higher carbon removal obligations in Canada. *Communications Earth & Environment*, *6*(1), 88. https://doi.org/10.1038/s43247-025-02080-z

Mulder, E. G., & Gerretsen, F. C. (1952). Soil Manganese in Relation to Plant Growth. In *Advances in Agronomy* (Vol. 4, pp. 221–277). Elsevier. https://doi.org/10.1016/S0065-2113(08)60310-7

Nelson, P. N., & Ham, G. J. (2000). Exploring the response of sugar cane to sodic and saline conditions through natural variation in the Field. *Field Crops Research*, *66*, 245–255. https://doi.org/10.1016/S0378-4290(00)00077-0

Nelson, P. N., & Su, N. (2010). Soil pH buffering capacity: A descriptive function and its application to some acidic tropical soils. *Soil Research*, *48*(3), 201–207. https://doi.org/10.1071/SR09150

Olego, M. A., Quiroga, M. J., Sánchez-García, M., Cuesta, M., Cara-Jiménez, J., & Garzón-Jimeno, J. E. (2021). Effects of overliming on the nutritional status of grapevines with special reference to micronutrient content. *OENO One*, *55*(2), 57–73. https://doi.org/10.20870/oeno-one.2021.55.2.4081

Parker, M. B., & Walker, M. E. (1986). Soil pH and Manganese Effects on Manganese Nutrition of Peanut. *Agronomy Journal*, *78*(4), 614–620. https://doi.org/10.2134/agronj1986.00021962007800040011x

Paulitz, T. C., & Schroeder, K. L. (2016). Acid Soils: How Do They Interact With Root Diseases? *FS195E*. Retrieved from https://pubs.extension.wsu.edu/product/acid-soils-how-do-they-interact-with-root-diseases-soil-acidification-series/

Pearson, R. W., Perez-Escolar, R., Abrufia, F., & Lund, Z. F. (1975). Comparative Response of Three Crop Species to Liming Several Soils of the Southeastern United States and of Puerto Rico. *Journal of Agriculture*.

Penn, C., & Camberato, J. (2019). A Critical Review on Soil Chemical Processes that Control How Soil pH Affects Phosphorus Availability to Plants. *Agriculture*, *9*(6), 120. https://doi.org/10.3390/agriculture9060120

Power, I. M., Hatten, V. N. J., Guo, M., Schaffer, Z. R., Rausis, K., & Klyn-Hesselink, H. (2025). Are enhanced rock weathering rates overestimated? A few geochemical and mineralogical pitfalls. *Frontiers in Climate*, 6:1510747. https://doi.org/10.3389/fclim.2024.1510747

Power, I. M., Spence, J., Guo, M., Wilson, S., & Watmough, S. (2026). Enhanced rock weathering has greater promise as a sustainable farming practice than a CO_2 removal technology. *Proceedings of the National Academy of Sciences*, *123*(26), e2602421123. https://doi.org/10.1073/pnas.2602421123

Puro.earth. (2025, December). Lithos Mid-West Facility (Lithos Carbon, Project 606367). Puro Registry. Retrieved from https://registry.puro.earth/projects/606367

Puro.earth. (2026, June). Chhattisgarh State (Mati Carbon, Project 868685). Puro Registry. Retrieved from https://registry.puro.earth/projects/868685

Ridley, A., Slattery, W., Helyar, K., & Cowling, A. (1990). The importance of the carbon cycle to acidification of a grazed annual pasture. *Australian Journal of Experimental Agriculture*, *30*(4), 529–537. https://doi.org/10.1071/EA9900529

Rogers, B., & Maher, K. (2026). A thermodynamic framework for lime requirement and alkalinity production in acidic soils. *Geoderma*, *473*, 117956. https://doi.org/10.1016/j.geoderma.2026.117956

Ruan, L., Li, J., Song, Z., Liu, C.-Q., Yu, C., Han, G., et al. (2026). Enhanced weathering for CO2 removal from a global perspective. *Carbon Research*, *5*(1), 66. https://doi.org/10.1007/s44246-026-00282-4

Saccardi, B. E., Dere, A. L., Goodwell, A. E., Druhan, J., Welp, L. R., Blair, N. E., et al. (2025). The scale of influence: How different drivers determine CO2 production at event, daily, and seasonal scales. *Frontiers in Water*, *7*, 1638541. https://doi.org/10.3389/frwa.2025.1638541

Schaber, T., Ekholm, T., Merikanto, J., & Partanen, A.-I. (2024). Prudent carbon dioxide removal strategies hedge against high climate sensitivity. *Communications Earth & Environment*, *5*(1), 285. https://doi.org/10.1038/s43247-024-01456-x

Sokol, N. W., Sohng, J., Moreland, K., Slessarev, E., Goertzen, H., Schmidt, R., et al. (2024). Reduced accrual of mineral-associated organic matter after two years of enhanced rock weathering in cropland soils, though no net losses of soil organic carbon. *Biogeochemistry*. https://doi.org/10.1007/s10533-024-01160-0

Steinwidder, L., Boito, L., Frings, P. J., Niron, H., Rijnders, J., De Schutter, A., et al. (2025). Beyond Inorganic C: Soil Organic C as a Key Pathway for Carbon Sequestration in Enhanced Weathering. *Global Change Biology*, *31*(7). https://doi.org/10.1111/gcb.70340

Strefler, J., Amann, T., Bauer, N., Kriegler, E., & Hartmann, J. (2018). Potential and costs of carbon dioxide

removal by enhanced weathering of rocks. *Environmental Research Letters*, *13*(3), 034010. https://doi.org/10.1088/1748-9326/aaa9c4

Strefler, J., Bauer, N., Humpenöder, F., Klein, D., Popp, A., & Kriegler, E. (2021). Carbon dioxide removal technologies are not born equal. *Environmental Research Letters*, *16*(7), 074021. https://doi.org/10.1088/1748-9326/ac0a11

Su, C., Kang, R., Driscoll, C. T., Zhu, W., Goll, D. S., Huang, W., et al. (2026). Overlooked Soil Acidity Leads to Significant Overestimation of Carbon Sequestration in Enhanced Rock Weathering. *Environmental Science & Technology*, *60*(32), 22505–22516. https://doi.org/10.1021/acs.est.6c05139

Suhrhoff, T. J., Dietzen, C., Kukla, T., Lunstrum, A., Reershemius, T., Thompson, J., et al. (2026, July). An Ecosystem of Carbon Dioxide Removal Reviews – Part 3: Enhanced Weathering. CDRXIV. https://doi.org/10.70212/cdrxiv.2026417.v1

Sumner, M. E., Farina, P. M. W., & Hurst, V. J. (1978). Magnesium fixation—a possible cause of negative yield responses to lime applications. *Communications in Soil Science and Plant Analysis*, *9*(10), 995–1007. https://doi.org/10.1080/00103627809366871

Swoboda, P., Döring, T. F., & Hamer, M. (2022). Remineralizing soils? The agricultural usage of silicate rock powders: A review. *Science of The Total Environment*, *807*, 150976. https://doi.org/10.1016/j.scitotenv.2021.150976

Te Pas, E. E. E. M., Chang, E., Marklein, A. R., Comans, R. N. J., & Hagens, M. (2025). Accounting for retarded weathering products in comparing methods for quantifying carbon dioxide removal in a short-term enhanced weathering study. *Frontiers in Climate*, *6*, 1524998. https://doi.org/10.3389/fclim.2024.1524998

Tsao, S. S.-E., Surhoff, T. J., Amatulli, G., Almaraz, M., Gewirtzman, J., Woollen, B., et al. (2025, September). A spatially explicit dataset of agriculture liming across the contiguous United States. ESSD – Land/Land cover and land use. https://doi.org/10.5194/essd-2025-411

Tu, Y., Rafols, R., Xu, Y., Butler, N., Ababneh, L., Tao, F., et al. (2026). Scaling up enhanced rock weathering for equitable climate change mitigation. *Communications Sustainability*, *1*(1), 32. https://doi.org/10.1038/s44458-026-00034-w

Vienne, A., Frings, P., Poblador, S., Steinwidder, L., Rijnders, J., Schoelynck, J., et al. (2024). Earthworms in an enhanced weathering mesocosm experiment: Effects on soil carbon sequestration, base cation exchange and soil CO2 efflux. *Soil Biology and Biochemistry*, *199*, 109596. https://doi.org/10.1016/j.soilbio.2024.109596

Vienne, A., Frings, P., Rijnders, J., Boito, L., Hartmann, J., Niron, H., et al. (2026). Weathering without realizing inorganic CO_2 removal revealed through base cation monitoring. *SOIL*, *12*(1), 421–440. https://doi.org/10.5194/soil-12-421-2026

Walker, R. L., Watson, C. A., & Edwards, A. C. (2015). Aspects of pH gradient effect on crop productivity and crop quality parameters in an eight course ley-arable rotation started in 1961. *Aspects of Applied Biology*, (128).

Waters, B. M., Amundsen, K., & Graef, G. (2018). Gene Expression Profiling of Iron Deficiency Chlorosis Sensitive and Tolerant Soybean Indicates Key Roles for Phenylpropanoids under Alkalinity Stress. *Frontiers in Plant Science*, *9*, 10. https://doi.org/10.3389/fpls.2018.00010

Winiwarter, V., & Blum, W. E. H. (2008). From marl to rock powder: On the history of soil fertility management by rock materials. *Journal of Plant Nutrition and Soil Science*, *171*(3), 316–324. https://doi.org/10.1002/jpln.200625070

Yonemura, S., Yokozawa, M., Shirato, Y., Nishimura, S., & Nouchi, I. (2009). Soil CO2 concentrations and their implications in conventional and no-tillage agricultural fields. *Journal of Agricultural Meteorology*, *65*(2), 141–149. https://doi.org/10.2480/agrmet.65.2.2

Zhang, T., Cui, J., Duan, X., Cui, D., Liu, X., Feng, Q., et al. (2023). Subsoiling reduces CO2 concentrations in soil profile of winter wheat – summer maize rotation ecosystem in the North China Plain: A strategy to achieve carbon neutrality in farmland. *Archives of Agronomy and Soil Science*, *69*(14), 2833–2846. https://doi.org/10.1080/03650340.2023.2175819

Zhu, Q., De Vries, W., Liu, X., Hao, T., Zeng, M., Shen, J., & Zhang, F. (2018). Enhanced acidification in Chinese croplands as derived from element budgets in the period 1980–2010. *Science of The Total Environment*, *618*, 1497–1505. https://doi.org/10.1016/j.scitotenv.2017.09.289